Fluid-solid equilibrium of carbon dioxide as obtained from computer simulations of several popular potential models: The role of the quadrupole

G. Pérez-Sánchez, D. González-Salgado, M. M. Piñeiro, and C. Vega

Citation: J. Chem. Phys. **138**, 084506 (2013); doi: 10.1063/1.4792443
View online: http://dx.doi.org/10.1063/1.4792443
View Table of Contents: http://jcp.aip.org/resource/1/JCPSA6/v138/i8
Published by the American Institute of Physics.

Fluid-solid equilibrium of carbon dioxide as obtained from computer simulations of several popular potential models: The role of the quadrupole

G. Pérez-Sánchez,[1,a)] D. González-Salgado,[2] M. M. Piñeiro,[1,b)] and C. Vega[3]
[1]*Departamento de Física Aplicada, Universidade de Vigo, 36310 Vigo, Spain*
[2]*Departamento de Física Aplicada, Universidade de Vigo, 32004 Ourense, Spain*
[3]*Departamento Química-Física I, Facultad de Ciencias Químicas, Universidad Complutense de Madrid, 28040 Madrid, Spain*

(Received 22 November 2012; accepted 4 February 2013; published online 25 February 2013)

In this work the solid-fluid equilibrium for carbon dioxide (CO_2) has been evaluated using Monte Carlo simulations. In particular the melting curve of the solid phase denoted as *I*, or dry ice, was computed for pressures up to 1000 MPa. Four different models, widely used in computer simulations of CO_2 were considered in the calculations. All of them are rigid non-polarizable models consisting of three Lennard-Jones interaction sites located on the positions of the atoms of the molecule, plus three partial charges. It will be shown that although these models predict similar vapor-liquid equilibria their predictions for the fluid-solid equilibria are quite different. Thus the prediction of the entire phase diagram is a severe test for any potential model. It has been found that the Transferable Potentials for Phase Equilibria (TraPPE) model yields the best description of the triple point properties and melting curve of carbon dioxide. It is shown that the ability of a certain model to predict the melting curve of carbon dioxide is related to the value of the quadrupole moment of the model. Models with low quadrupole moment tend to yield melting temperatures too low, whereas the model with the highest quadrupole moment yields the best predictions. That reinforces the idea that not only is the quadrupole needed to provide a reasonable description of the properties in the fluid phase, but also it is absolutely necessary to describe the properties of the solid phase. © *2013 American Institute of Physics*. [http://dx.doi.org/10.1063/1.4792443]

I. INTRODUCTION

Carbon dioxide (CO_2) is undoubtedly one of the most relevant and widely studied molecules. It is a common solvent in chemical engineering,[1–3] widely used in the food industry and also increasingly used in new processes, for instance, the synthesis of ultra-hard materials in materials science.[4] It plays a key role in biological processes such as photosynthesis, respiration, and participates in the global carbon cycle. The time evolution of its concentration in the atmosphere has become a matter of primary interest worldwide. The environmental concerns related to the control and management of anthropogenic emissions of green house gases have set the focus of society, industry, and scientists on this molecule as one of the hottest global issues, due to the connection between its atmospheric concentration and climate change. For this reason, research on CO_2 capture,[5] reutilization, and long term storage has increased continuously and is expected to continue, because feasible and efficient technical solutions for these questions are still not available and represent an urgent need. The interest in CO_2 is not limited to the fluid phase and their mixtures.[6–12] In fact, in the last decade, our knowledge of the solid phases of CO_2 has increased significantly thanks to a number of experimental and theoretical studies.[13–26] Today it is believed that the solid phase of CO_2 comprises of seven different polymorphs. At temperatures and pressures lower than 800 K and 12 GPa, respectively, we can find the solid phase *I*, usually named *dry ice*, belonging to the cubic Pa3 space group.[27,28] Increasing pressure at moderate temperatures (lower than 500 K), the phase *III* is reached which is an orthorhombic structure[28,29] (space group Cmca). Both phases are of molecular nature, i.e., the structure of the CO_2 molecule in these solid phases is basically that of the molecule in the gas phase.[30] On increasing temperature, in the pressure interval from 20 GPa to 40 GPa, approximately, two different solid phases are formed, labelled as *II* and *IV*, whose molecular[17,21,31,32] or non-molecular[33–35] character is matter of debate. At very high pressures, phases *V*,[4,20,22] *VI*,[14] and a-carbonia,[15] three strictly non-molecular solids can be found in which the intermolecular interactions are fully covalent. In addition, a new molecular phase (phase *VII*[31]) was obtained at pressure close to 12 GPa and at temperatures around 800 K. In summary even though CO_2 is a simple molecule its phase diagram is rather complex, and it seems an interesting test to analyze whether simple molecular models can describe such a complex behavior.

In molecular studies carbon dioxide is usually described by using a linear rigid model with three interaction sites. The three sites are located approximately on the positions of the atoms of the molecule. Typically each of the sites contains a Lennard-Jones (LJ) center and a partial charge. Obviously a rigid empirical model cannot describe the formation of solids where the molecule of carbon dioxide dissociates into its atoms (i.e., a non-molecular solid). In this case true electronic structure calculations such as density functional theory

a)Present address: Universidade do Porto, Portugal.
b)Electronic mail: mmpineiro@uvigo.es.

(DFT) are probably the only alternative. However, it seems of interest to analyze whether these models can provide a reasonable description of the phase diagram in the region of low temperature and pressure where carbon dioxide remains as a molecular solid. Before addressing this interesting issue, it seems reasonable to study an even simpler question: can simple molecular models of CO_2 reproduce the melting point of its simplest solid phase *I* (dry ice)? Notice that potential parameters are usually obtained to reproduce the vapor-liquid equilibria[36–38] and their capacity to reproduce the experimental melting point of dry ice should not be taken for granted. Also it seems obvious that a model that simultaneously describes the vapor-liquid and the liquid-solid equilibria seems superior to one that only describes the fluid phase properly. In this work we shall determine the melting point of the solid phase *I* for four popular models of CO_2. In particular we have selected the MSM model[39–41] (named after the initials of the authors of the original paper), and some recent updates such as EPM2[42] (a variation of the original EPM, standing for Elementary Physical Model), TraPPE[43] (Transferable Potentials for Phase Equilibria), and the recent model by Zhang and Duan.[44] The differences between these models are the values of the characteristic LJ interaction parameters and electric charges for each site, and the carbon-oxygen bond length. It will be shown that the best results are obtained when using the TraPPE,[43] showing that there is at least a model describing quite well the vapor-liquid and the liquid-solid equilibria.

It is of interest to connect the behavior of CO_2 to that of another simple molecule: water. Water also presents a complex phase diagram and over the last few years it has been shown that models that predict reasonably well the vapor-liquid equilibria may fail completely when predicting the phase diagram and/or the melting point. This observation has been useful in the design of improved water potentials, and also it has clarified the key role played by the quadrupole moment when describing water properties.[45–48] Carbon dioxide has no dipole moment, but has a significant quadrupole moment. It will be shown here that the quadrupole moment also plays a key role for understanding the melting point of a molecular model.

II. METHODOLOGY

In this work some of the most popular CO_2 molecular models have been considered. The MSM model, the first in chronological order, was defined by using experimental data of gas phase, *ab initio* calculations, and lattice parameters of the solid state. The rest of the models, EPM2, TraPPE, and Zhang and Duan, are considered as descendants of the former. In these cases, however, experimental thermophysical properties were used in their parameterizations. Thus, EPM2 was developed in order to accurately predict the vapor liquid equilibria (VLE) of pure carbon dioxide, TraPPE was fitted to VLE data of the mixture CO_2 with propane, whereas Zhang and Duan model tried to improve the previous predictions of the VLE data of pure CO_2. The interaction between molecule *i* and *j* is given by

$$u_{ij} = \sum_a \sum_b u_{ab}, \tag{1}$$

$$u_{ab} = 4\varepsilon_{ab}\left(\left(\frac{\sigma_{ab}}{r_{ab}}\right)^{12} - \left(\frac{\sigma_{ab}}{r_{ab}}\right)^{6}\right) + \frac{q_a q_b}{r_{ab}}, \tag{2}$$

where u_{ab} and r_{ab} are the energy and the distance between site *a* of molecule *i* and site *b* of molecule *j*, respectively, ε_{ab} and σ_{ab} are the LJ parameters, and q_a and q_b are the partial charges. The internal energy *U* for a system of *N* molecules is determined from the intermolecular energy between the *i*th and *j*th molecule u_{ij},

$$U = \sum_{i=1}^{N} \sum_{j>i}^{N} u_{ij}. \tag{3}$$

The parameters of the potential for these four models are presented in Table I. For each force field the LJ parameters and partial charges located on each atom are provided. In addition, the resulting value of the quadrupole moment is presented. Unlike interactions have been described using the Lorentz-Berthelot combining rules. It is fair to say that in spite of small differences the four models considered present similar values for the CO bond length and σ (differences being typically below five percent). The most significant difference between the models is the value of the partial charge located on the carbon atom (since the molecule is electroneutral this is sufficient to determine the partial charge on the oxygen atoms). Differences in the value of partial charge can be of up to 20%–25% and this is reflected in the value of the quadrupole moment. The values of ϵ are not so different, but in general, the larger the charge located on the C atom, the lower the value of the epsilon parameters. Since these models provide relatively similar vaporization enthalpies, the key difference between them is the different weight of dispersive (as given by ϵ) to Coulombic interactions (as given by the partial charges and the quadrupole moment). The Zhang model presents large dispersive interactions and small quadrupolar interactions. The TraPPE model presents smaller dispersive interactions and higher quadrupolar interactions. It seems

TABLE I. Lennard-Jones parameters for each model used in this work. Parameters between different particles follows the Lorentz-Berthelot rules. l_{c-o} is the distance between carbon and oxygen particle in the CO_2 molecule and *Q* is the molecular quadrupolar moment in $D \times$ Å, where $1D \times$ Å $= 3.336 \times 10^{-40}$ C $\times$ m^2.

Models	ε_{c-c}/k (K)	σ_{c-c} (Å)	ε_{o-o}/k (K)	σ_{o-o} (Å)	q_c (e)	l_{c-o} (Å)	Q ($D \times$ Å)
Zhang	28.845	2.792	82.656	3.000	0.5888	1.163	3.18
MSM	29.000	2.785	83.100	3.014	0.5957	1.160	3.20
EPM2	28.129	2.757	80.507	3.033	0.6512	1.149	3.44
TraPPE	27.000	2.800	79.000	3.050	0.7000	1.160	3.78

interesting to study if the melting point would be sensitive or not to such a different balance between dispersive and Coulombic forces.

Let us describe briefly the procedure used to determine the fluid-solid (I) coexistence line for each model. The procedure has been described elsewhere[49–51] so we shall provide here only a brief description. For a certain selected pressure/s, the temperature at which the chemical potential of the two phases (liquid and solid) becomes identical is determined. This provides an initial coexistence point. The entire coexistence line can be obtained by using the Gibbs-Duhem (GD) integration method proposed by Kofke.[52–54] This method consists in the numerical integration of the Clapeyron equation,

$$\frac{dp}{dT} = \frac{s_{II} - s_I}{v_{II} - v_I} = \frac{h_{II} - h_I}{T(v_{II} - v_I)}, \tag{4}$$

where I and II represent the two coexisting phases and we use lower case for thermodynamic properties per molecule. The integration of this equation can be achieved using different methods. In the particular case where the slope in the $p - T$ plane is pronounced, an alternative calculation method is advised. In this work, the equations to be integrated have been $dT/dp = T\Delta v/\Delta h$ for the solid-fluid coexistence line, and $d \ln p/d\beta$, where $\beta = 1/(kT)$ for the case of fluid-vapor coexistence. In both cases the integration has been solved numerically using a fourth order Runge-Kutta algorithm, and the determination of the enthalpy and volume variations between the coexisting phases was obtained performing isotropic NpT simulations.

It remains to be explained how the initial coexistence point where both phases have the same chemical potential is located. First, the chemical potential is calculated for the desired pressure at a certain reference temperature. The chemical potential is given by

$$\mu/kT = G/(NkT) = A/(NkT) + pV/(NkT). \tag{5}$$

Once the chemical potential at the reference state is known, we shall perform thermodynamic integration to determine the chemical potential along the considered isobar. This is done for both the fluid and solid phases. After this is done it is rather simple to locate the temperature at which both phases have the same chemical potential for the considered pressure. The tricky aspect of the calculation is that although the pV/NkT is easily evaluated for the reference state from NpT runs, the evaluation the Helmholtz free energy A is more involved. For the solid phase we shall use the Einstein molecule method to determine A_{sol}. In this methodology the solid of interest is transformed into an ideal Einstein molecule for which the free energy is known easily using analytical and simple numerical methods. The ideal Einstein molecule is a system where no intermolecular interactions are present and each molecule is connected through translational and orientational harmonic springs to the solid lattice configuration except one molecule whose translational move is forbidden. We refer the readers to a previous review on the topic,[50] and to our previous work on methanol for further details.[55,56] The expression for A_{sol} from the Einstein molecule method is given by

$$A_{sol} = A_{Ein-mol-id} + \Delta A_1^* + \Delta A_2^* = A_0^* + \Delta A_1^* + \Delta A_2^*, \tag{6}$$

where $A_{Ein-mol-id}$ (or A_0^*) is the free energy of the ideal Einstein molecule, ΔA_1^* is the free energy change between the ideal Einstein molecule with intermolecular interactions and the ideal Einstein molecule, both with molecule 1 fixed (i.e., fixing its center of mass) and, ΔA_2^* is the free energy change between the solid with molecule 1 fixed and the interacting ideal Einstein molecule with molecule 1 fixed. The system energy due to the harmonic springs follows the next expressions:

$$U_{Ein-mol-id,t} = \sum_{i=2}^{N} \Lambda_E (\Delta r_i)^2, \tag{7}$$

$$U_{Ein-mol-id,r} = \sum_{i=1}^{N} \Lambda_{Eb} \sin^2(\psi_{b,i}), \tag{8}$$

where Λ_E and Λ_{Eb} are the spring constants, Δr_i is the vector connecting the position of an atom of molecule i (i.e., the carbon atom) in the current position to that of this atom in the ideal solid reference lattice and $\psi_{b,i}$ is the angle formed between the C–O vector of molecule i in the current configuration and that of the C–O vector in the ideal solid reference lattice. The Einstein molecule method cannot be used for the fluid phase. In this case A_{liq} was determined by using thermodynamic integration and assuming ideal gas behavior for the gas phase at 800 K and 0.1 MPa.

Finally let us provide some further details about the NpT and NVT simulations performed in this work. The initial configuration for the solid was a Pa3 structure unit cell,[28] composed by four molecules whose disposition and orientation have been represented in Figure 1. The Pa3 space group is a cubic crystalline structure, and this simplifies the calculations because the simulations of the solid phase as those of the fluid can be performed using NpT simulations with isotropic

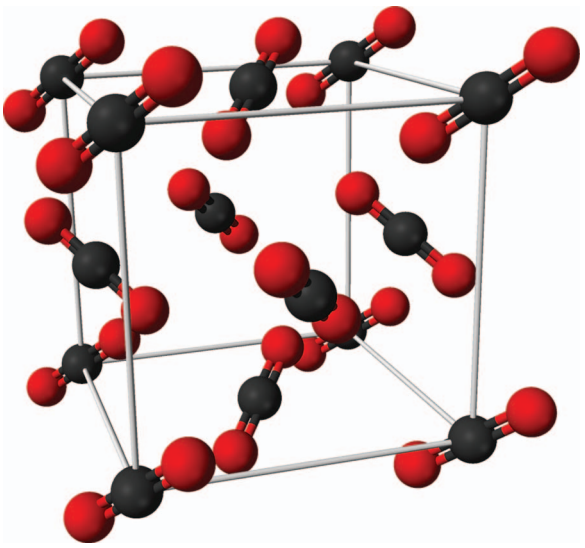

FIG. 1. Unit cell of carbon dioxide in the cubic Pa3 solid structure denoted as dry ice.

scaling. The initial lattice parameter of the solid phase was $a = 5.54$ Å. This cell has been replicated four times in the three spatial directions to obtain a simulation box containing $N = 256$ molecules. Notice that initial value of the lattice parameter a has no influence on the calculations as the system finds (in the NpT simulations) its equilibrium value at a certain T and p for the considered model. Simulations were arranged in cycles, each of them consisting of N attempts to move or rotate a molecule chosen at random, plus a volume change trial in the case of NpT simulations. Maximum molecule displacements, rotations, and volume changes were tuned along the simulation to approach a 30% acceptance ratio. In a recent paper, Frenkel[57] has recalled, among many other interesting aspects concerning molecular simulation, the mathematical reasoning supporting the choice of acceptance ratio values around 30%, related with the optimization of sampling efficiency for Metropolis-style Monte Carlo (MC) moves. A cut off radius of 10 Å for solid and fluid phases and $1/5L$, in the case of 800 K isotherm at pressures of 0.1, 1, 5, and 10 MPa, have been considered where L is the size of the simulation box. Apart from the usual LJ long range corrections,[58] the Ewald summation method[59] was used for the Coulombic interactions. For NVT and NpT, solid and fluid phases, the simulation runs were first a equilibration stage of 20 000 cycles followed by production runs of typically 40 000 cycles. In the case of Gibbs-Duhem simulations, the equilibration and the production runs were of 10 000 cycles.

The selection of number of molecules and simulation runs length deserves an additional comment before proceeding further. Several authors have used the Gibbs-Duhem integration algorithm to determine solid-liquid equilibria along molecular simulation calculations, and the number of particles used is in many cases much larger than the one used here. For instance, Ahmed and Sadus[60] used this technique to determine the Weeks-Chandler-Andersen potential phase diagram, by simulating 4000 molecules using molecular dynamics, with the objective to avoid finite size effects. The same authors determined the system size dependence for the solid-fluid equilibria calculation for the Gaussian core model fluid,[61] determining the optimal system size to be 2048 molecules, a value which was used again later for the same calculation in the case of the n-6 LJ potentials family.[62] In addition, they discussed also the effects of potential truncation and shift for the solid fluid equilibria calculations for the case of the LJ potential.[63] In the present work, and with the aim to discard the possible influence of finite size effects, additional calculations were performed for a system containing 500 molecules. The coincidence in the numerical values of the properties determined was remarkable, with density variations typically in the fifth significative digit, and Helmholtz free energy variations in the fourth figure, which leads to equilibrium temperatures according to within the statistical uncertainty with the values shown in the tables. The same comparison procedure was performed with simulation runs twice longer, with identical results. This underlines the robustness of the method used that will be supported also by the agreement of triple point coordinates obtained by other authors for different CO_2 models using different simulation techniques and system sizes.

TABLE II. Helmholtz free energy of the solid phase A_{sol} as evaluated from Einstein molecule calculations at 100 K for different pressures. Free energy calculations were obtained in NVT runs at the equilibrium density of the system at 100 K and the considered pressure. The maximum value of the spring constant was 25 000 (in $kT/Å^2$ for the translational spring and in kT units for the orientational one). The thermal deBroglie wavelength was assigned to 1 Å.

	A_{sol}/NkT		
Models	1000 MPa	200 MPa	4 MPa
Zhang	−21.57	−22.72	−22.80
MSM	−21.71	−22.88	−22.96
EPM2	−22.48	−23.62	−23.70
TraPPE	−23.78	−24.92	−25.00

III. RESULTS

The free energy of the solid phase at 100 K (for the pressures 1000 MPa, 200 MPa, and 4 MPa) as obtained from Einstein molecule calculations is presented in Table II. The reason for performing three independent free energy calculations for each model is as follows: in principle the evaluation of the free energy for only one pressure (in combination with thermodynamic integration), would be sufficient to determine the free energy along the isotherm. However, performing three independent calculations allows to perform a consistency check. Starting from the value evaluated at 1000 MPa and performing thermodynamic integration one should obtain the same free energy at 200 MPa and 4 MPa than that obtained from the Einstein molecule methodology. This is a severe test. In Table III free energies at 200 MPa and 4 MPa are presented as obtained from Einstein molecule calculations and as obtained from thermodynamic integration starting from the free energy computed at 1000 MPa. The small differences between both sets of values is remarkable, ensuring the consistency between both calculation methods. Since free energy calculations for solids are somewhat involved, these consistency tests are highly recommended. It is interesting to compare the free energies obtained at 100 K and 200 MPa (conclusions would be similar for other pressures) obtained for the different models. As can be seen the free energy of the Zhang and MSM are quite similar, being the results for the EPM2 model lower by approximately 1 NkT , and those of the TraPPE model lower by 2 NkT. Thus for the TraPPE model the solid phase I is about 2 NkT more stable than for the Zhang and/or MSM models. It is interesting to point out that in the I solid structure

TABLE III. Helmholtz free energies in NkT units, A_{EM} and A_{TI}, obtained by Einstein molecule method (EM) and thermodynamic integration (TI), respectively, for the potential models considered in this work, at $T = 100$ K.

	200 MPa		4 MPa	
Models	A_{EM}	A_{TI}	A_{EM}	A_{TI}
Zhang	−22.72	−22.73	−22.80	−22.81
MSM	−22.88	−22.89	−22.96	−22.97
EPM2	−23.62	−23.63	−23.70	−23.71
TraPPE	−24.92	−24.92	−25.00	−25.00

TABLE IV. Helmholtz free energies A_{fluid} of the fluid phase at the thermodynamic reference points. The A_{fluid} value at 1000 MPa and 200 MPa was evaluated by using thermodynamic integration along the $T = 800$ K isotherm from ideal gas state (0.1 MPa). An additional thermodynamic integration along an isochore was needed to obtain the A_{fluid} value at 4 MPa. The density of the isochore was set to the density value of each model at 4 MPa and 250 K. Temperature of 800 K for 1000 and 200 MPa pressures and 250 K for 4 MPa pressure.

	A_{fluid}/NkT		
Models	1000 MPa	200 MPa	4 MPa
Zhang	−3.48	−5.18	−7.59
MSM	−3.48	−5.18	−7.63
EPM2	−3.46	−5.17	−7.63
TraPPE	−3.45	−5.17	−7.76

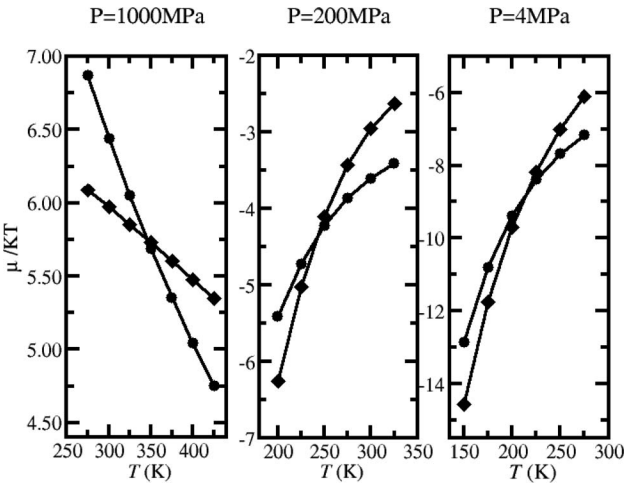

FIG. 2. Chemical potential μ as a function of temperature T obtained from the TraPPE model for the solid (◆) and fluid (●) phases for the three isobars investigated.

(also denoted as αN_2 in the literature) the relative orientation between first nearest neighbors is T like.[64] Not surprisingly this is the most stable relative orientation for a pair of ideal quadrupoles. Thus it is clear that the larger value of the quadrupole moment of the TraPPE model[43] is playing a key role in the stabilization of the solid phase. Although this is interesting, these results by themselves do not guarantee that the melting point of the TraPPE model will be higher than that of the MSM and/or Zhang models. It may also be the case that for the fluid phase the free energy of the TraPPE model is lower than that of the Zhang model by the same amount, and in such a case both models would have the same melting point temperature. To analyze this in more detail the free energy for the fluid phase has been calculated at several pressures. Results are presented in Table IV. Under the considered conditions the free energies of the four models are quite similar. Therefore, the higher quadrupole of the TraPPE model has a much smaller impact in the fluid free energies. It is interesting to point out that the average energy between two quadrupoles is zero when the molecules are able to rotate freely.[64] Of course molecules in the fluid phase do not behave as free rotors, but it is clear that orientational correlations are much smaller in the fluid than in the solid phase (in this last case first nearest neighbors must adopt a T like configuration in the I solid). For a given fluid, one would expect that if the models predict the same vapor-liquid coexistence curve, they should also produce the same liquid phase free energies. The partitioning of energies between LJ (dispersive) and Coulombic interactions is largely irrelevant for weakly/non-associating fluids as long as the overall magnitude and range of the interactions is correct. Some extreme examples demonstrate this: Avendaño *et al.*[65] have developed a single site CO_2 model (not considering the quadrupole) as part of the SAFT-γ approach that provides a very good reproduction of the fluid phase properties; and Ketko and Potoff[66] have developed a series of models for dimethyl ether using a wide range of partial charges (including zero) that reproduce in all cases the saturated liquid densities to within 1%–2% of experimental values. While these aforementioned models are able to reproduce the fluid phase properties to high accuracy, they would obviously provide poor predictions of solid-liquid coexistence.

From the discussion presented so far one may anticipate that the TraPPE model will present a higher melting temperature for a given pressure, and that the ordering of the melting temperatures will be given by the order of the quadrupole moment. Now we shall determine the fluid-solid equilibria for several pressures. Once the chemical potential is known for a reference state within each isobar then thermodynamic integration can be performed along the isobar to obtain the chemical potential as a function of the temperature. When this is done for the fluid and solid phases, the coexistence is simply found as the temperature at which the chemical potential of both phases becomes identical for each considered pressure. For the solid phase, thermodynamic integration was performed using the results of NpT simulations along the isobars of 1000, 200, and 4 MPa. These NpT simulations were performed by increasing the temperature starting from the initial reference temperature (i.e., 100 K) for which chemical potential is known. Similarly for the fluid phase thermodynamic integration was performed using the results of NpT simulations along the isobars 1000, 200, and 4 MPa. These NpT simulations were performed by decreasing the temperature starting from the initial reference temperature (i.e., 800 K, for 1000 MPa and 200 MPa, 250 K for 4 MPa) for which chemical potential of the fluid phase is known. Figure 2 plots the chemical potential values obtained for the TraPPE model, for both the fluid and the solid phases. For each pressure the intersection point determines the coexistence temperature. Table V lists the coexistence point temperatures determined for each model at different pressures. Bearing in mind the quadrupole moment values for each model listed in Table I, an inspection of Table V reveals a direct correlation between these values and the estimated coexistence temperature at a given pressure. In fact, the models in Table V are ordered in increasing Q values, starting with Zhang and Duan model, the one with the lowest Q value, up to TraPPE model. The results of Table V do indeed confirm the relation between the melting point and the quadrupole moment, a relation already anticipated from the analysis of the free energies.

TABLE V. Solid-fluid coexistence points for each model at different pressures. Last two columns show the triple point temperature and pressure obtained for each model along with the experimental value.[69] All temperatures are in Kelvin.

Models	1000 MPa	200 MPa	4 MPa	T_t	p_t (MPa)
Zhang	290	216	189	188	0.136
MSM	298	217	189	188	0.130
EPM2	321	232	200	200	0.123
TraPPE	345	249	214	213	0.44
Expt.	...	...	...	216.6	0.518

Once the fluid-solid equilibria have been determined for at least one pressure one can use Gibbs-Duhem integration to obtain the entire melting curve. We have used the coexistence temperature at the pressure of 1000 MPa as the initial coexistence point. Since one single coexistence point is sufficient to obtain the entire melting curve, the calculation of the coexistence conditions for three different points may appear to be excessive. However, it offers an important advantage. It allows once again to cross-check all the calculations. In fact, by using GD integration and starting from the coexistence point at a certain pressure one should reproduce the coexistence conditions for other pressures obtained from free energy calculations (provided that there is no error in the calculations). Figure 3 plots the estimated solid-fluid coexistence lines in a $T - p$ diagram for the models considered in this work. Experimental results for the melting curve are also presented.[67] The conclusion is clear. The TraPPE model provides an excellent description of the experimental melting curve of CO_2. It is important to emphasize that the TraPPE model was not designed to reproduce the melting curve, so that its success in the prediction is a true merit of the model. The GD lines presented in Figure 3 started at 1000 MPa. The lines are entirely consistent with the coexistence points estimated at 200 MPa and 4 MPa from free energy calculations. That shows the consistency of the calculations. Let us now focus on the location of the vapor-liquid-solid triple point.

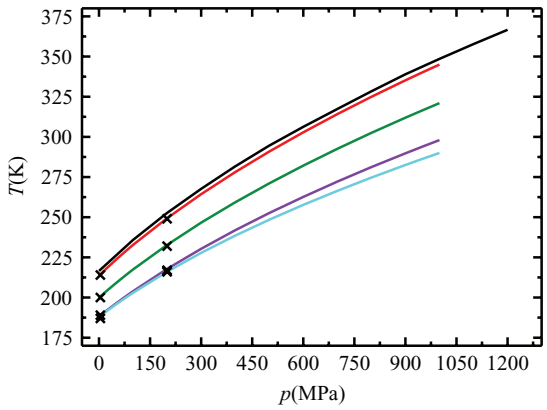

FIG. 3. Solid-fluid coexistence lines in the $T - p$ diagram for each model as obtained from Gibbs-Duhem simulations starting from the coexistence point at 1000 MPa: TraPPE (red line), EPM2 (green line), MSM (violet line), and Zhang (cyan line), compared with experimental data[67] (black line). Symbols represent coexistence points obtained from independent free energy calculations.

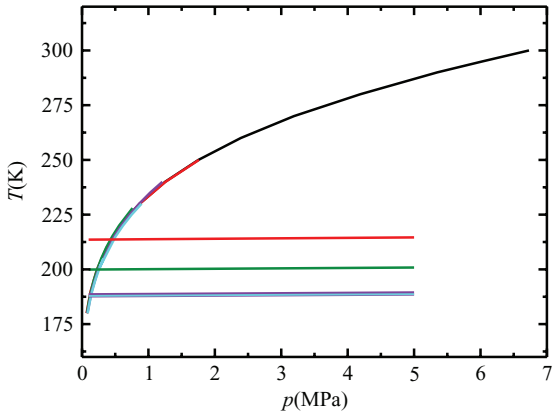

FIG. 4. Solid-fluid and fluid-vapor coexistence lines for each model compared with experimental data.[68] Legend as in Figure 3.

The triple point can be simply determined by representing the vapor-liquid and fluid-solid coexistence curves on a $T - p$ plot. The intersection of both lines yields the triple point temperature and pressure. In Figure 4 the vapor-liquid coexistence curves and fluid-solid curves are presented. The vapor-liquid coexistence line was obtained using the Gibbs-Duhem method from specific coexistence points taken from Refs. 42–44. The fluid-solid coexistence curves appears as approximately horizontal lines indicating that changing the pressure by a few MPa does not modify much the melting temperature. The upper part of the graph represents the vapor-liquid coexistence pressure (i.e., the vapor pressure curve) obtained for the models and compared with experimental data.[68] Obviously in this case a change of a few MPa significantly modifies the coexistence temperature. It is clear that all models considered in this work predict similar (and accurate) vapor-pressures. For this reason the vapor pressure curves for the four models considered in this work show excellent agreement with the experimental results. However the melting curves are quite different. Consequently the triple point conditions (i.e., the intersection of the two coexistence curves) are quite different for each model. The triple point coordinates, are listed in Table V along with the experimental results.[69] The TraPPE model provides excellent predictions not only for the triple point temperature, but also for the triple point pressure. Notice that the triple point pressure of the TraPPE is approximately three times higher than that of the other models. The TraPPE model predicts quite well not only the triple point temperature and pressure but also the density of the phases at the triple point. This is shown more clearly in Table VI.

TABLE VI. Densities of the solid, fluid, and vapor at the triple point conditions of each model. Experimental results are also shown.[68]

	ρ(g cm^{-3})		
Models	Solid	Fluid	Vapor
Zhang	1.537	1.270	0.004
MSM	1.527	1.261	0.004
EPM2	1.524	1.225	0.006
TraPPE	1.501	1.181	0.012
Experiment	1.512	1.178	0.013

It is interesting to compare the numerical values of the triple point coordinates obtained in this work with results from other authors, obtained using also molecular simulation, and the TraPPE molecular model for CO_2, but different calculation techniques and simulation settings. For instance, Chen *et al.*[70] determined the triple point coordinates, using Gibbs Ensemble MC simulations, for a system containing a total of 1728 molecules, to study the coexistence of solid and vapor phases, yielding values of $T_t = 212 \pm 2$ K and $P_t = 0.45 \pm 0.05$ MPa, which are fully consistent with the values obtained here. Recently, Do and Wheatley[71] proposed a novel simulation density of states partitioning technique, intended to calculate the free energy of a solid phase. It is to be noted that their calculations were performed with 500 molecules, and the TraPPE CO_2 triple point coordinate estimates were $T_t = 213 \pm 2$ K and $P_t = 0.41 \pm 0.03$ MPa, again in very good accordance with our values. The conclusion obtained from this comparison deserves to be commented upon. The agreement shown between the triple point coordinates for the TraPPE CO_2 model, obtained using different simulation techniques and system sizes ranging from 256 to 1728 molecules underlines the reliability of the calculation method applied in each of the cases cited. Although it is well known that finite size effects play an important role in solid-fluid equilibria determination using molecular simulation, as demonstrated by Ahmed and Sadus,[60] and the further study of the thermodynamic limit of these "realistic" models of CO_2 is an interesting goal, the results of this work compared with the other two references cited[70,71] evidence that the triple point of the TraPPE model of CO_2 for the typical system size used in computer simulations is located around $T_t = 212$ K.

Once the fluid-solid curve has been determined for each model it is interesting to compare the predictions for the melting enthalpy with the experimental values.[67] This is done in Figure 5. All models underestimate the melting enthalpy. That said the results of the TraPPE model are closer to the experimental values. Since the melting enthalpy increases with the value of the quadrupole moment the results of Figure 5 suggest that an important contribution to the melting enthalpy of carbon dioxide is due to the quadrupolar interaction energy. Further work is needed to understand why all models of carbon dioxide underestimate the melting enthalpy. Volume changes along the fluid-solid coexistence curve are shown in Figure 6. The results are similar to those for the melting enthalpy. All models underestimate the volume change, the results of the TraPPE model being much closer to the experimental values. The symbols shown in Figures 5 and 6 were obtained by performing long *NpT* runs (50 000 cycles) of the fluid and solid phase at four selected values of the coexistence line. The symbols are quite close to the results obtained from Gibbs-Duhem simulations (lines) which were obtained using somewhat shorter runs. Therefore, the underestimate of the melting enthalpy and volume change of the four considered models is a real effect.

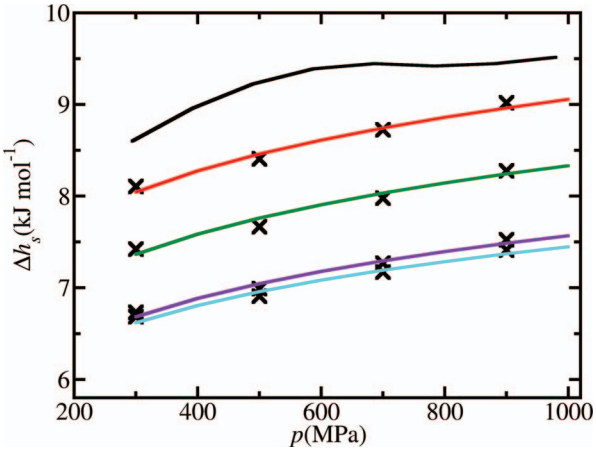

FIG. 5. Melting enthalpy Δh_s at different pressures for all tested models compared to experimental data[67] (legend as in Figure 3). Symbols represent results for simulations at 300, 500, 700, and 900 MPa carried out to check the Gibbs-Duhem results.

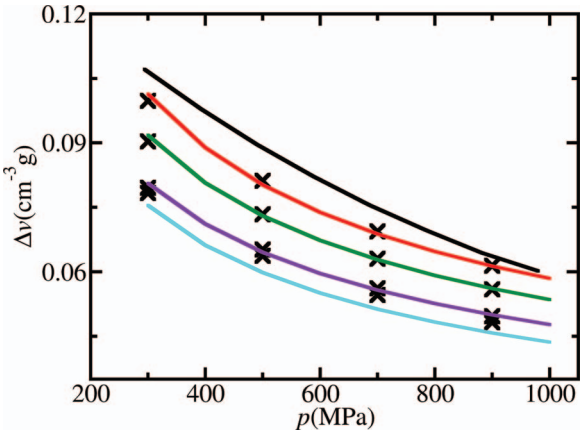

FIG. 6. Melting volumes Δv_s at different pressures. Legend as in Figure 5.

We have also studied the mechanical stability of the solid along several the 1000, 200, and 4 MPa isobars. We found that in general dry ice was mechanically stable up to temperatures of 100 K (1000 MPa), 70 K (200 MPa), and 50 K (4 MPa) above the equilibrium melting temperature for each considered pressure. That means that the carbon dioxide solid (in absence of interface) can be overheated in *NpT* simulations. This is in line with previous results for water, where it was found that in computer simulations (without interfaces) ices could be superheated by about 70–80 K with respect to the equilibrium melting temperature.[72]

IV. CONCLUSIONS

In this work the fluid-solid coexistence and triple points have been located for four popular models of carbon dioxide. These four models yield quite reasonable predictions of the vapor-liquid equilibria. This is not surprising as vapor-liquid equilibria are commonly used as a target property when determining the parameters of most forcefields. However, the four models yield quite different predictions for the triple point (vapor-liquid-solid) conditions and for melting curves. Thus the prediction of the entire phase diagram (including also fluid-solid equilibria) is a severe test for potential models. It is clear from the results of this work that the TraPPE model yields an overall better performance of the phase diagram of carbon dioxide. It fact, it predicts the triple point

temperature and pressure quite well, and the same is true for the melting curve. It also yields reasonable estimates (although the agreement with experiment is not yet fully quantitative) for the melting enthalpy and for the volume change along the melting curve.

It is interesting to analyze the origin of the superiority of the TraPPE model. Already in the 1970s and 1980s it was known that adding an ideal quadrupole to a spherical simple model (i.e., HS, LJ) modified significantly the structure of the liquid phase.[73,74] Several studies also analyzed its impact on the critical properties.[75–79] The conclusion of these studies was that the quadrupole significantly affected the fluid properties, including the vapor-liquid equilibria. Since experimentally carbon dioxide presents an important quadrupole it seems reasonable to incorporate the quadrupole in the model. However, it should be reminded that even without the quadrupole it is still possible to provide quite reasonable estimate of the properties in the fluid phase.[65,80] But when it comes to the solid phase, the role of the quadrupole is not needed just to improve the phase equilibria predictions, but it is absolutely required to understand its phase diagram. Some time ago it was shown that for a simple linear model without quadrupole moment the stable phase is not the αN_2 structure (i.e., ice *I*). This solid phase was stable only when the quadrupole was introduced in the model.[81] Later on it was shown that to understand the small liquid range of carbon dioxide (as reflected by the parameter T_t/T_c which adopts an extraordinary high value for CO_2) a high value of the quadrupole moment is needed.[82,83] The four models considered in this work do indeed have a quadrupole moment. But its magnitude changes significantly from one model to another. Since all models provide reasonable values of the vaporization enthalpy, it means that the relative weight of dispersive to Coulombic forces is different in the four models. It turns out that the model with the highest quadrupole moment (TraPPE) is also the model with the best prediction of the triple point temperature and pressure. The TraPPE model is the model that has a quadrupole moment closest to the value estimated by Vrabec *et al.*[84] and to the experimental value in the gas phase. In some recent studies the key role played by the quadrupole to understand the phase diagram of water, and also the correlation between the melting temperature and the quadrupole moment for ice I_h has been illustrated.[45–47] It seems that the same is true for carbon dioxide. Quadrupolar forces (and polar forces in general) depend quite significantly of the relative orientation between molecules. In the solid phases of molecular solids, these relative orientations are dictated by the geometry of the lattice. It is not surprising then that the solid phase is far more sensitive to the quadrupole moment than the fluid phase.[85] It is shown here, that TraPPE does indeed a good job and its good performance is related to its high quadrupole moment. It seems clear that to understand the properties of carbon dioxide, one must not only include some Coulombic interactions, but its strength must also be correct. There is not much hope in describing the phase diagram of carbon dioxide without taking into account its high quadrupole moment. Whether the TraPPE model is successful in describing other solid phases of carbon dioxide (those that can be regarded as molecular solids since TraPPE can never describe the molecular dissociation as it is a rigid model) is an issue that probably deserves future studies.

ACKNOWLEDGMENTS

The authors acknowledge CESGA (www.cesga.es), for providing access to computing facilities, Consellería de Educación e Ordenación Universitaria and Proj. CN2012/227 (Xunta de Galicia), Ministerio de Ciencia e Innovación (Proj. Refs. FIS2009-07923, FIS2010-16159, FIS2011-29614 and FIS2012-33621), and Univ. de Vigo (Proj. 11VIA16), all in Spain, for financial support.

[1] G. Brunner, *Gas Extraction* (Springer, New York, 1991).
[2] K. Mishima, K. Matsuyama, D. Tanabe, S. Yamauchi, T. J. Young, and K. P. Johnston, AIChE J. **46**, 857 (2000).
[3] W. Leitner, Acc. Chem. Res. **35**, 746 (2002).
[4] C.-S. Yoo, H. Cynn, F. Gygi, G. Galli, V. Iota, M. Nicol, S. Carlson, D. Hausermann, and C. Mailhiot, Phys. Rev. Lett. **83**, 5527 (1999).
[5] N. MacDowell, N. Florin, A. Buchard, J. Hallett, A. Galindo, G. Jackson, C. S. Adjiman, C. K. Williams, N. Shah, and P. Fennell, Energy Environ. Sci. **3**, 1645 (2010).
[6] L. F. Vega, O. Vilaseca, F. Llovell, and J. S. Andreu, Fluid Phase Equilib. **294**, 15 (2010).
[7] A. Dias, H. Carrier, J. L. Daridon, J. C. Pamies, L. F. Vega, J. A. P. Coutinho, and I. M. Marrucho, Ind. Eng. Chem. Res. **45**, 2341 (2006).
[8] F. Llovell and L. F. Vega, J. Phys. Chem. B **110**, 1350 (2006).
[9] T. Lafitte, B. Mendiboure, M. M. Piñeiro, D. Bessières, and C. Miqueu, J. Phys. Chem. B **114**, 11110 (2010).
[10] J. M. Míguez, M. C. dos Ramos, M. M. Piñeiro, and F. J. Blas, J. Phys. Chem. B **115**, 9604 (2011).
[11] B. M. Mognetti, M. Oettel, P. Virnau, L. Yelash, and K. Binder, Mol. Phys. **107**, 331 (2009).
[12] K. Binder, Mol. Phys. **108**, 1797 (2010).
[13] J. Sun, D. D. Klug, R. Martonak, J. A. Montoya, M.-S. Lee, S. Scandolo, and E. Tosatti, Proc. Natl. Acad. Sci. U.S.A. **106**, 6077 (2009).
[14] V. Iota, C.-S. Yoo, J.-H. Klepeis, Z. Jenei, W. Evans, and H. Cynn, Nature Mater. **6**, 34 (2007).
[15] M. Santoro, F. A. Gorelli, R. Bini, G. Ruocco, S. Scandolo, and W. A. Crichton, Nature (London) **441**, 857 (2006).
[16] T. Kume, Y. Ohya, M. Nagata, S. Sasaki, and H. Shimizu, J. Appl. Phys. **102**, 053501 (2007).
[17] F. A. Gorelli, V. M. Giordano, P. R. Salvi, and R. Bini, Phys. Rev. Lett. **93**, 205503 (2004).
[18] O. Tschauner, H.-K. Mao, and R. J. Hemley, Phys. Rev. Lett. **87**, 075701 (2001).
[19] V. Iota and C.-S. Yoo, Phys. Status Solidi **223**, 427 (2001).
[20] V. Iota, C.-S. Yoo, and H. Cynn, Science **283**, 1510 (1999).
[21] S. A. Bonev, F. Gygi, T. Ogitsu, and G. Galli, Phys. Rev. Lett. **91**, 065501 (2003).
[22] M. Santoro, J. F. Lin, H. K. Mao, and R. J. Hemley, J. Chem. Phys. **121**, 2780 (2004).
[23] B. Holm, R. Ahuja, A. Belonoshko, and B. Johansson, Phys. Rev. Lett. **85**, 1258 (2000).
[24] S. Serra, C. Cavazzoni, G. L. Chiarotti, S. Scandolo, and E. Tossati, Science **284**, 788 (1999).
[25] M. Santoro and F. A. Gorelli, Chem. Soc. Rev. **35**, 918 (2006).
[26] V. M. Giordano and F. Datchi, Phys. Rev. Lett. **99**, 165701 (2007).
[27] B. Olinger, J. Chem. Phys. **77**, 6255 (1982).
[28] B. Kuchta and R. D. Etters, Phys. Rev. B **38**, 6265 (1988).
[29] R. C. Hanson, J. Chem. Phys. **89**, 4499 (1985).
[30] K. E. Anderson, S. L. Mielke, J. I. Siepmann, and D. G. Truhlar, J. Phys. Chem. A **113**, 2053 (2009).
[31] V. M. Giordano and F. Datchi, Europhys. Lett. **77**, 46002 (2007).
[32] F. Datchi, V. M. Giordano, P. Munsch, and A. M. Saitta, Phys. Rev. Lett. **103**, 185701 (2009).
[33] C.-S. Yoo, V. Iota, and H. Cynn, Phys. Rev. Lett. **86**, 444 (2001).
[34] V. Iota and C.-S. Yoo, Phys. Rev. Lett. **86**, 5922 (2001).
[35] C.-S. Yoo, H. Kohlmann, H. Cynn, M. F. Nicol, V. Iota, and T. LeBihan, Phys. Rev. B **65**, 104103 (2002).
[36] A. Z. Panagiatopoulos, Mol. Phys. **61**, 813 (1987).

[37]A. Z. Panagiatopoulos, N. Quirke, M. Stapleton, and D. J. Tildesley, Mol. Phys. **63**, 527 (1988).
[38]B. Smit, P. de Smedt, and D. Frenkel, Mol. Phys. **68**, 931 (1989).
[39]C. S. Murthy, K. Singer, and I. R. McDonald, Mol. Phys. **44**, 135 (1981).
[40]L. C. Geiger, B. M. Ladanyi, and M. E. Chapi, J. Chem. Phys. **93**, 4533 (1990).
[41]C. S. Murthy, S. F. Oshea, and I. R. M. Donald, Mol. Phys. **50**, 531 (1983).
[42]J. G. Harris and K. H. Yung, J. Phys. Chem. **99**, 12021 (1995).
[43]J. J. Potoff and J. I. Siepmann, AIChE J. **47**, 1676 (2001).
[44]Z. Zhang and Z. Duan, J. Chem. Phys. **122**, 214507 (2005).
[45]J. L. F. Abascal and C. Vega, Phys. Chem. Chem. Phys. **9**, 2775 (2007).
[46]J. L. F. Abascal and C. Vega, Phys. Rev. Lett. **98**, 237801 (2007).
[47]J. L. F. Abascal and C. Vega, J. Phys. Chem. C **111**, 15811 (2007).
[48]C. Vega and J. L. F. Abascal, Phys. Chem. Chem. Phys. **13**, 19663 (2011).
[49]D. Frenkel and A. J. C. Ladd, J. Chem. Phys. **81**, 3188 (1984).
[50]C. Vega, E. Sanz, J. L. F. Abascal, and E. G. Noya, J. Phys. Condens. Matter **20**, 153101 (2008).
[51]E. G. Noya, M. M. Conde, and C. Vega, J. Chem. Phys. **129**, 104704 (2008).
[52]D. A. Kofke, J. Chem. Phys. **98**, 4149 (1993).
[53]D. A. Kofke, Mol. Phys. **78**, 1331 (1993).
[54]D. A. Kofke, "Semigrand canonical Monte Carlo simulation: Integration Along coexistence lines," in *Monte Carlo Methods in Chemical Physics*, edited by D. M. Ferguson, J. L. Siepmann, and D. G. Truhlar (Wiley, New York, 1998), Vol. 105, p. 404.
[55]D. G. Salgado and C. Vega, J. Chem. Phys. **132**, 094505 (2010).
[56]D. González-Salgado, A. Dopazo-Paz, P. Gómez-Alvarez, J. M. Míguez, and C. Vega, J. Phys. Chem. B **115**, 3522 (2011).
[57]D. Frenkel, "Simulations: the dark side," arXiv:1211.4440v1 [cond-mat.stat-mech] (2012).
[58]M. P. Allen and D. J. Tildesley, *Computer Simulation of Liquids* (Oxford University Press, Oxford, 1987).
[59]D. Frenkel and B. Smit, *Understanding Molecular Simulation* (Academic, New York, 2002).
[60]A. Ahmed and R. J. Sadus, Phys. Rev. E **80**, 061101 (2009).
[61]P. Mausbach, A. Ahmed, and R. J. Sadus, J. Chem. Phys. **131**, 184507 (2009).
[62]A. Ahmed and R. J. Sadus, J. Chem. Phys. **131**, 174504 (2009).
[63]A. Ahmed and R. J. Sadus, J. Chem. Phys. **133**, 124515 (2010).
[64]C. G. Gray and K. E. Gubbins, *Theory of Molecular Fluids* (Clarendon, Oxford, 1984).
[65]C. Avendaño, T. Lafitte, A. Galindo, C. S. Adjiman, G. Jackson, and E. A. Muller, J. Phys. Chem. B **115**, 11154 (2011).
[66]M. B. H. Ketko and J. J. Potoff, Mol. Simul. **33**, 769 (2007).
[67]P. W. Bridgman, Phys. Rev. **3**, 126 (1914).
[68]R. Span and W. Wagner, J. Phys. Chem. Ref. Data **25**, 1509 (1996).
[69]S. Angus, B. Armstrong, and K. M. de Reuck, *International Thermodynamic Tables of the Fluid State. 3. Carbon Dioxide, International Union of Pure and Applied Chemistry* (Pergamon Press, New York, 1976).
[70]B. Chen, J. I. Siepmann, and M. L. Klein, J. Phys. Chem. B **105**, 9840 (2001).
[71]H. Do and R. J. Wheatley, J. Chem. Theory Comput. **9**, 165 (2013).
[72]C. McBride, C. Vega, E. Sanz, L. G. MacDowell, and J. L. F. Abascal, Mol. Phys. **103**, 1 (2005).
[73]G. N. Patey and J. P. Valleau, J. Chem. Phys. **64**, 170 (1976).
[74]S. L. Carnie and G. N. Patey, Mol. Phys. **47**, 1129 (1982).
[75]M. R. Stapleton, D. J. Tildesley, A. Z. Panagiotopoulos, and N. Quirke, Mol. Simul. **2**, 147 (1989).
[76]B. Garzón, S. Lago, C. Vega, E. de Miguel, and L. F. Rull, J. Chem. Phys. **101**, 4166 (1994).
[77]S. F. O'Shea, G. S. Dubey, and J. C. Rasaiah, J. Chem. Phys. **107**, 237 (1997).
[78]A. L. Benavides, Y. Guevara, and A. F. Estrada-Alexanders, J. Chem. Thermodyn. **32**, 945 (2000).
[79]A. L. Benavides, S. Lago, B. Garzón, L. F. Rull, and F. del Río, Mol. Phys. **103**, 3243 (2005).
[80]B. M. Mognetti, L. Yelash, P. Virnau, W. Paul, K. Binder, M. Muller, and L. G. MacDowell, J. Chem. Phys. **128**, 104501 (2008).
[81]C. Vega and P. A. Monson, J. Chem. Phys. **102**, 1361 (1995).
[82]E. P. A. Paras, C. Vega, and P. A. Monson, Mol. Phys. **79**, 1063 (1993).
[83]C. Vega and P. A. Monson, Mol. Phys. **85**, 413 (1995).
[84]J. Vrabec, J. Stoll, and H. Hasse, J. Phys. Chem. B **105**, 12126 (2001).
[85]J. W. Schroer and P. A. Monson, J. Chem. Phys. **114**, 4124 (2001).